

# Recovering inhomogeneities in a waveguide using eigensystem decomposition

Sava Dediú and Joyce R. McLaughlin

Department of Mathematical Sciences, Rensselaer Polytechnic Institute, 110 8th Street, Troy, NY 12180-3590, USA

E-mail: dedius2@rpi.edu, mcclauj@rpi.edu

**Abstract.** We present an eigensystem decomposition method to recover inhomogeneities in a waveguide from knowledge of the far-field scattered acoustic fields. Due to the particular geometry of the waveguide, which supports only a finite number of propagating modes, the problem of recovering inhomogeneities in a waveguide has a different set of challenges than its corresponding problem in free space. Our method takes advantage of the spectral properties of the far-field matrix, and by using its eigenvalues and its eigenvectors we obtain a representation of the linearized solution to the inverse problem in terms of products of fields which are linear combinations of the propagating modes of the waveguide with weights given by the eigenvectors of the far-field matrix. The problem of finding the unknown inhomogeneity reduces to a problem of determining some coefficients in a finite system of linear equations whose coefficients depend on the background medium and the eigenvalues and the eigenvectors of the far-field matrix. By numerically implementing our inverse algorithm we reconstructed the inhomogeneities present in the waveguide. We show that: (1) even with as few as seven propagating modes we obtain a good recovery of the size and shape of the inhomogeneity; (2) multiple inhomogeneities can be well recovered; and, as expected, (3) the recovery improves when the number of propagating modes increases.

## 1. Introduction

In this paper, we present a new method to determine the index of refraction in a compact inhomogeneous region in a waveguide with known background from measurements of the far-field scattered acoustic waves. What is new about our problem relative to a standard inverse scattering problem in free space is that we have only a finite number of propagating modes. It is thus important to develop a method that optimally utilizes this essentially different feature. Our method exploits the spectral properties of the far-field operator, which is determined by the measured data, and for the waveguide problem effectively reduces to a matrix. The problem of finding the unknown inhomogeneity is shown to reduce to a problem of determining some coefficients in a finite system of linear equations whose coefficients depend on the background medium and the eigenvalues and the eigenvectors of the far-field matrix.

The problem of reconstructing the index of refraction in acoustical waveguides has received considerable attention in the last years and is motivated by practical applications in Ocean Acoustics where one wants to localize and identify inhomogeneities submerged in shallow waters. Of the areas of practical interest where our method may have potential applications we mention:

- commercial fishery (where one wants to locate and characterize schools of fish);
- marine ecology (with important applications in ecosystem and food chain surveillance, biomass estimation for fish and zooplankton swarms, governmental control of fishing quota, nutrients transport etc);
- imaging of the seabed (localization of industrial waste and sand bank accumulations with applications in ecological survey and cleanup operations in harbors).

The problem of determining a distributed inhomogeneity in a shallow ocean from scattered acoustic waves was previously considered in [8], [9], [10] and [21]. In most cases, the shallow ocean is modeled by a two-layered waveguide of an ocean over a fluid-like seabed. The physical problem is formulated as a boundary value problem: the equation inside the waveguide is the Helmholtz equation, and at the top and the bottom of the waveguide, acoustically soft and respectively acoustically hard boundary conditions are imposed. The inhomogeneity to be reconstructed is modeled as a smooth, small perturbation in the background wavenumber and it is located in either one of the two layers: in [8], [9], and [21] it is located in the water column, whereas in [10] it is considered to be buried in the seabed. Assuming that the acoustical properties of the waveguide background are known, the authors present an algorithm to reconstruct the unknown inhomogeneity by sending in incident waves from point sources located on a horizontal line and detecting the total waves along another horizontal line. Both lines are assumed to be located above the inhomogeneity. For given measured data the inverse problem is then reformulated as an overdetermined linear system and by using a regularization method, the authors obtain a minimization problem which they solve for the approximate solution.

Our approach for the inverse waveguide problem was inspired by an idea of Mast, Nachman and Waag [17] for the free space problem, where eigenfunctions of the scattering operator are used to generate fields which focus energy onto the support of the inhomogeneity. A regularized solution to the nonlinear inverse scattering problem is shown to result from combinations of products of these fields. Although at a high level our approach is similar to the one in [17], there are important differences due to the different characteristics of the waveguide problem. In [17], one illuminates the inhomogeneity with incident ultrasound plane waves evenly distributed over  $M$  angles between 0 and  $2\pi$  and the scattered fields are also measured at  $M$  receivers evenly distributed around the inhomogeneity, which results in a *full aperture* data for the free space inverse scattering problem. Moreover, for each fixed frequency, the number  $M$  of incident plane waves/receivers can be arbitrarily increased which yields richer data sets and therefore better reconstructions for the same central frequency. For our waveguide problem the measured data set is severely reduced, since at low frequency (the regime we are considering in this paper, and imposed by the applications we are targeting) there is only a small number of propagating modes. We should also mention that although there are no receivers below or above the inhomogeneity, our reconstructions are enhanced by the reflections of the scattered field from the top and the bottom of the waveguide.

Our paper is organized as follows. In Section 2, we introduce a mathematical model for our physical problem based on Helmholtz equation and appropriate boundary and radiation conditions. In Section 3 we study the asymptotic behavior of the scattered fields, and we show that at large distances from the inhomogeneous region, the scattered fields reduce to weighted superpositions of propagating modes. In

Sections 4 and 5 we define the scattering amplitude and respectively the far-field matrix for our waveguide problem, and we prove that the scattering amplitude satisfies a reciprocity relation similar to the one encountered in the free space problem and in the case of a nonabsorbent medium, the far-field matrix is normal with respect to a weighted inner product. In Section 6, we use the eigenvalues and the eigenvectors of the far-field matrix to obtain a representation of the linearized solution to the inverse problem in terms of products of fields which are linear combinations of the propagating modes of the waveguide with weights given by the eigenvectors of the far-field matrix. Using the data generated by a fourth order finite difference solver for the direct problem, in Section 7 we numerically implement our inverse algorithm and we reconstruct the inhomogeneities present in the waveguide. We show that: (1) even with as few as seven propagating modes we obtain a good recovery of the size and shape of the inhomogeneity; (2) multiple inhomogeneities can be well recovered; and, as expected, (3) the recovery improves when the number of propagating modes increases. Finally, in Section 8 we give our conclusions.

## 2. The Mathematical Model for the Direct Problem

We assume that we have a two-dimensional water-filled waveguide, infinite in the  $x$ -direction (range direction) and of depth  $D$  in the  $z$ -direction ( $z$ -direction pointing downward). In the middle of the waveguide, we assume that we have an inhomogeneous region of compact support, penetrable by acoustical waves and having a different sound speed than that of the background medium which surrounds it (See Fig. 1). The sound speed of the background medium depends only on depth, i.e.  $c = c(z)$ . Inside the inhomogeneous region, the sound speed depends on both range and depth, i.e.  $c = c(x, z)$ .

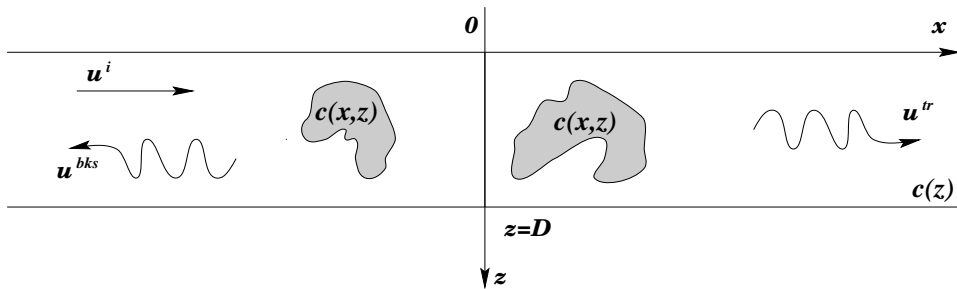


Figure 1. Wave propagation and scattering in a waveguide

In the interior of the waveguide, the equation governing the propagation of waves at fixed frequency is the Helmholtz equation

$$\Delta u + \frac{\omega^2}{c^2(x, z)} u = 0, \quad (2.1)$$

where  $u = u^i + u^s$ , is the *total field* for our problem, representing the superposition of the *incident field*  $u^i$  used to probe the waveguide, and the *scattered field*  $u^s$  which is generated when the incident field passes through the inhomogeneous region. The wavenumber  $\omega/c(x, z)$  is assumed to be real and continuous. The assumption that the wavenumber is real implies that we model a *nonabsorbent* medium. The assumption

to be continuous was made only for convenience, and is not an essential constraint. The water-air interface at the surface of the ocean and the water-rock interface at the bottom are modeled by acoustically soft and respectively acoustically hard boundary conditions

$$u = 0 \quad \text{at} \quad z = 0, \quad (2.2)$$

$$u_z = 0 \quad \text{at} \quad z = D. \quad (2.3)$$

When one sends an incident field through a waveguide which contains inhomogeneities, the resultant scattered field has two components: a transmitted field and a backscattered field. Both of these fields are outgoing, that is in time they move away from the inhomogeneous region. In mathematical terms, this is equivalent to the fact that the scattered field  $u^s$  satisfies the following radiation condition

$$u_\nu^s(L, z) = Qu^s(L, z) \quad \text{at} \quad x = \pm L, \quad (2.4)$$

where  $u_\nu(L, z)$  represents the normal derivative of  $u$  at  $x = \pm L$ , and  $L > 0$  is large enough such that the inhomogeneous region lies inside  $\Omega = [-L, L] \times [0, D]$ . The operator  $Q$  is the Dirichlet-to-Neumann operator for our problem, given by

$$Q = \sum_{n=1}^{\infty} i\sqrt{\lambda_n} \psi_n(z) (\cdot, \psi_n)_{L^2(0,D)}, \quad (2.5)$$

where  $(\lambda_n, \psi_n)$  are the eigenvalues and the eigenfunctions of the Sturm-Liouville problem

$$\psi''(z) + \frac{\omega^2}{c^2(z)} \psi(z) = \lambda \psi(z), \quad (2.6)$$

$$\psi(0) = \psi'(D) = 0. \quad (2.7)$$

The eigenfunctions  $\{\psi_n(z)\}_{n \geq 1}$  are real-valued, orthogonal and they form a complete system in  $L^2(0, D)$ . Without loss of generality, we will consider them normalized, i.e.,  $\|\psi_n\|_{L^2} = 1$ . The second derivative operator  $d^2/dz^2$  in (2.6) is negative definite, implying that all its eigenvalues are negative and approaching  $-\infty$ . But the positive term  $\omega^2/c^2(z)$  will shift these eigenvalues to the right, making the first few of them positive and thus dividing the sequence  $\{\lambda_n\}_{n \geq 1}$  of eigenvalues for the Sturm Liouville problem (2.6)-(2.7) in two parts:

$$\lambda_1 > \lambda_2 > \dots > \lambda_N > 0 > \lambda_{N+1} > \lambda_{N+2} > \dots > \lambda_{N+k} > \dots > -\infty,$$

i) a first part which is finite and contains only the positive eigenvalues ( $n = 1, \dots, N$ ), and ii) a second part which is infinite and contains all the remaining negative eigenvalues ( $n = N + 1, \dots, \infty$ ). It is important to mention that for our analysis in the sequel, we use the convention that the square root of a negative real number has a positive imaginary part, i.e.  $Im\sqrt{\lambda_n} > 0$  if  $\lambda_n < 0$  and  $\sqrt{\lambda_n} > 0$  if  $\lambda_n > 0$ .

Using Green's theorem, one can easily establish that the direct scattering problem (2.1)-(2.4) is equivalent to the problem of solving the integral equation

$$u(x, z) = u^i(x, z) + \int_{\Omega} G(x, z; X, Z) q(X, Z) u(X, Z) dXdZ, \quad (2.8)$$

also known as the *Lippman-Schwinger equation*. Here  $G$  is the Green's function for the unperturbed waveguide problem due to a unit point source located at  $(X, Z)$

$$G(x, z; X, Z) = \sum_{n=1}^{\infty} \frac{1}{2i\sqrt{\lambda_n}} e^{i\sqrt{\lambda_n}|x-X|} \psi_n(z) \psi_n(Z), \quad (2.9)$$

and  $q(x, z)$

$$q(x, z) = \frac{\omega^2}{c^2(z)} - \frac{\omega^2}{c^2(x, z)}, \quad (2.10)$$

is *the variation in the sound speed or the scattering potential* for our waveguide problem. The potential  $q$  represents the perturbation of the acoustic properties of the inhomogeneous region from the acoustic properties of the background medium. It is important to note that  $q$  is nonzero only on the support of the inhomogeneous region inside  $\Omega$ , and is zero elsewhere.

At this point, we introduce *the inverse problem we address in this paper*, which we formulate as follows: Given incident fields  $\{u^i\}$  and the acoustic properties of the background medium ( $\omega/c(z)$  is assumed to be known), find the potential  $q(x, z)$  when the scattered fields  $\{u^s\}$  are assumed to be known from measurements on two vertical lines at the opposite openings of the waveguide.

Since the scattered fields  $\{u^s\}$  are the part of the solutions that contain information about the location, the shape and the acoustic properties of an unknown inhomogeneity hidden in a waveguide, they naturally constitute our starting point of investigation.

### 3. Analysis of the Forward Problem: The Asymptotic Form of the Scattered Field

We start by deriving the asymptotic form of the scattered field  $u^s$  in the *far field*, that is at large distances from the inhomogeneous region which generates it. This analysis will give us the approximate analytical form of the field which we measure on the two vertical lines at the openings of the waveguide. But more importantly, it will help us *identify the relevant information about our inhomogeneity* which remains encrypted in the scattered field after all the decaying processes which occur during its propagation through the waveguide. We will extract this information, analyze it, and use it to derive an algorithm for our inverse problem, as we will see in the sequel.

However, before starting any analysis with respect to the scattered field and its asymptotic form, the first question to ask is: What would be an appropriate incident field to send through the waveguide?

There are a number of papers in the literature ([8], [9], [10], [21]), where it is assumed that the waveguide is excited by a point source, and the scattered field is measured on a horizontal line located above the inhomogeneity. Here, we use a different framework, and we assume that we illuminate the waveguide with incident fields consisting of propagating modes of the waveguide, i.e. modes which correspond to positive eigenvalues  $\lambda_m$

$$u_{\pm m}^i = e^{\pm i\sqrt{\lambda_m}x} \psi_m(z) \quad m = 1, \dots, N \quad (3.1)$$

coming both from the left and from the right side, and we measure the resultant scattered fields on two vertical lines located at the openings of the waveguide. We note that the propagating modes represent a natural choice for the incident fields, because they satisfy automatically the unperturbed Helmholtz equation, the boundary conditions (2.2) and (2.3) and they behave like plane waves in the  $x$  direction. Since in the time domain the propagating modes are multiplied by  $e^{-i\omega t}$ , an incident field with a positive index in (3.1) represents a propagating mode from the left to the right, whereas one with a negative index represents a propagating mode from the right to

the left. We use the convention throughout this paper that a positive index represents a mode (or a quantity associated with a mode) which travels from the left to the right, and a negative index represents a mode (or a quantity associated with a mode) which travels from the right to the left.

Regardless of the direction the incident propagating mode  $u^i$  is coming from, the corresponding scattered field  $u^s$  always has two outgoing components: a component outgoing to plus infinity and another one to minus infinity. By substituting (2.9) in (2.8), we obtain that the asymptotic form of the scattered field  $u_m^s$  corresponding to the incident propagating mode  $u_{\pm m}^i$  is

$$u_{\pm m}^s(x, z) = \begin{cases} \sum_{n=1}^N \frac{1}{2\sqrt{\lambda_n i}} e^{i\sqrt{\lambda_n} x} \psi_n(z) A_n^{\pm m} + O(e^{-\sqrt{|\lambda_{N+1}|}|x|}) & \text{for } x \gg L \\ \sum_{n=1}^N \frac{1}{2\sqrt{\lambda_n i}} e^{-i\sqrt{\lambda_n} x} \psi_n(z) A_{-n}^{\pm m} + O(e^{-\sqrt{|\lambda_{N+1}|}|x|}) & \text{for } x \ll -L, \end{cases} \quad (3.2)$$

where

$$A_{\pm n}^{\pm m} = \int_{\Omega} e^{\mp i\sqrt{\lambda_n} X} \psi_n(Z) q(X, Z) [e^{\pm i\sqrt{\lambda_m} X} \psi_m(Z) + u_{\pm m}^s(X, Z)] dX dZ, \quad (3.3)$$

(see [6]). As expected, in (3.2) we obtain the asymptotic expansion of the two components of the scattered field only in terms of the propagating modes of the waveguide (modes corresponding to the positive eigenvalues), the energy transferred to the evanescent modes decaying exponentially fast. By their nature, the propagating modes which appear in (3.2) do not contain any information about the inhomogeneity present in the waveguide. They represent just the *propagating eigenmodes of the unperturbed waveguide*, traveling freely from one opening to the other. As one can see in (3.3), the information about our inhomogeneity contained in  $u_{\pm m}^s$  is transferred to the coefficients  $A_n^{\pm m}$  and  $A_{-n}^{\pm m}$ , which can be interpreted as the *projection* of  $q(X, Z)[e^{i\sqrt{\lambda_m} X} \psi_m(Z) + u_m^s(X, Z)]$  onto the propagating modes  $u_{\pm m}(x, z) = e^{\pm i\sqrt{\lambda_m} x} \psi_m(z)$  (see (2.8) and (2.9)). Because of this property, these coefficients are extremely important for our inverse method, and we will build our inverse algorithm based on them.

#### 4. Analysis of the Forward Problem: The Reciprocity Relation of the Scattering Amplitude

We now define the scattering amplitude for our waveguide problem in a natural way, by collecting the coefficients of the propagating modes which appear in the asymptotic expansion of the scattered fields (3.2), and arranging them in a column vector. We call the vector  $\mathcal{A}^m$  given by:

$$\mathcal{A}^m = \begin{bmatrix} \frac{1}{2\sqrt{\lambda_1 i}} A_1^m \\ \frac{1}{2\sqrt{\lambda_2 i}} A_2^m \\ \vdots \\ \frac{1}{2\sqrt{\lambda_N i}} A_N^m \\ \frac{1}{2\sqrt{\lambda_1 i}} A_{-1}^m \\ \frac{1}{2\sqrt{\lambda_2 i}} A_{-2}^m \\ \vdots \\ \frac{1}{2\sqrt{\lambda_N i}} A_{-N}^m \end{bmatrix} = \frac{1}{2i} \Lambda^{-1} \begin{bmatrix} A_1^m \\ A_2^m \\ \vdots \\ A_N^m \\ A_{-1}^m \\ A_{-2}^m \\ \vdots \\ A_{-N}^m \end{bmatrix} \quad (4.1)$$

the *scattering amplitude* or the *far-field pattern* corresponding to the  $m^{\text{th}}$  incident propagating mode ( $m = \pm 1, \dots, \pm N$ ). Here  $N$  is the number of propagating modes and  $\Lambda$  is the diagonal matrix

$$\Lambda = \text{diag} \left[ \sqrt{\lambda_1}, \sqrt{\lambda_2}, \dots, \sqrt{\lambda_N}, \sqrt{\lambda_1}, \sqrt{\lambda_2}, \dots, \sqrt{\lambda_N} \right]. \quad (4.2)$$

Each scattering amplitude is a  $2N$  column vector corresponding to an incident propagating mode. Since we illuminate the waveguide with  $N$  incident modes coming from each side (both left and right), we have a total of  $2N$  scattering amplitudes. We show next that these scattering amplitudes satisfy a reciprocity relation similar to the one encountered in the free space case.

**Theorem 1** (*Reciprocity Relation*) *The scattering amplitude satisfies the following reciprocity relation*

$$A_n^m = A_{-m}^{-n} \quad (\text{transmitted part}) \quad (4.3)$$

$$A_{-n}^m = A_{-m}^n \quad (\text{left backscattered part}) \quad (4.4)$$

$$A_n^{-m} = A_m^{-n} \quad (\text{right backscattered part}) \quad (4.5)$$

for all  $m, n = 1, \dots, N$ .

The physical interpretation and the proof of this theorem can be found in [6], where is also remarked that (4.3)-(4.5) hold in general for all  $m, n = 1, \dots, \infty$ .

## 5. Analysis of the Forward Problem: The Normality of the Far Field Matrix

Consider all the far-field patterns  $\mathcal{A}^m$ , for  $m = \pm 1, \dots, \pm N$ . We collect them in the matrix  $\mathcal{A}$  given by:

$$\mathcal{A} = \frac{1}{2i} \Lambda^{-1} \begin{bmatrix} A_1^1 & A_1^2 & \dots & A_1^N & \left| & A_1^{-1} & A_1^{-2} & \dots & A_1^{-N} \right. \\ A_2^1 & A_2^2 & \dots & A_2^N & \left| & A_2^{-1} & A_2^{-2} & \dots & A_2^{-N} \right. \\ \vdots & \vdots & & \vdots & \left| & \vdots & \vdots & & \vdots \\ A_N^1 & A_N^2 & \dots & A_N^N & \left| & A_N^{-1} & A_N^{-2} & \dots & A_N^{-N} \right. \\ A_{-1}^1 & A_{-1}^2 & \dots & A_{-1}^N & \left| & A_{-1}^{-1} & A_{-1}^{-2} & \dots & A_{-1}^{-N} \right. \\ A_{-2}^1 & A_{-2}^2 & \dots & A_{-2}^N & \left| & A_{-2}^{-1} & A_{-2}^{-2} & \dots & A_{-2}^{-N} \right. \\ \vdots & \vdots & & \vdots & \left| & \vdots & \vdots & & \vdots \\ A_{-N}^1 & A_{-N}^2 & \dots & A_{-N}^N & \left| & A_{-N}^{-1} & A_{-N}^{-2} & \dots & A_{-N}^{-N} \right. \end{bmatrix} \quad (5.1)$$

which we call the *far-field matrix* for our waveguide problem. Using the reciprocity relations (4.3)-(4.5), we show that in the case of a nonabsorbent medium, the far-field matrix  $\mathcal{A}$  is normal with respect to the weighted inner product

$$\langle x, y \rangle = \sum_{n=1}^N \sqrt{\lambda_n} x_{-n} \bar{y}_{-n} + \sum_{n=1}^N \sqrt{\lambda_n} x_n \bar{y}_n = x^T \Lambda y. \quad (5.2)$$

Before proceeding to the main result of this section we need the following auxiliary lemma, whose proof can also be found in [6].

**Lemma 1** *In the case of a nonabsorbent medium, the far-field matrix  $\mathcal{A}$  satisfies*

$$\langle \alpha, \mathcal{A}\beta \rangle + \langle \mathcal{A}\alpha, \beta \rangle + \langle \mathcal{A}\alpha, \mathcal{A}\beta \rangle = 0 \quad (5.3)$$

for all  $\alpha$  and  $\beta$  in  $\mathbb{C}^{2N}$ .

We state and prove now the main result of this section:

**Theorem 2** *In the case of a nonabsorbent medium, the far-field matrix  $\mathcal{A}$  is normal with respect to the weighted inner product (5.2).*

**Proof:** We rewrite the far-field matrix  $\mathcal{A}$  as a block matrix:

$$\mathcal{A} = \frac{1}{2i}\Lambda^{-1}A = \frac{1}{2i}\Lambda^{-1} \begin{bmatrix} A^{LR} & A^{RR} \\ A^{LL} & A^{RL} \end{bmatrix}$$

where:  $A^{LR}$  is the scattering amplitude block corresponding to incident waves sent from the left and scattered fields measured to the right;  $A^{RR}$  is the backscattering amplitude block corresponding to incident waves sent from the right and backscattered fields measured to the right;  $A^{LL}$  is the backscattering amplitude block corresponding to incident waves sent from the left and backscattered fields measured to the left; and finally  $A^{RL}$  is the scattering amplitude block corresponding to incident waves sent from the right and scattered fields measured to the left. From the reciprocity relations satisfied by the scattering amplitude, we have that:

$$A^{LR} = (A^{RL})^T \quad A^{LL} = (A^{LL})^T \quad A^{RR} = (A^{RR})^T. \quad (5.4)$$

The adjoint of the matrix  $\mathcal{A}$  with respect to the weighted inner product (5.2) is  $\mathcal{A}^* = \Lambda^{-1}\overline{\mathcal{A}^T}\Lambda$ . Using the identities (5.4), we have that for an incident wave distribution  $\alpha = [\alpha_1, \alpha_2, \dots, \alpha_N, \alpha_{-1}, \alpha_{-2}, \dots, \alpha_{-N}]^T = [\alpha_+, \alpha_-]^T$ ,  $\mathcal{A}^*\alpha$  is given by

$$\begin{aligned} \mathcal{A}^*\alpha &= -\frac{1}{2i}\Lambda^{-1}\overline{A^T}\alpha = \overline{\frac{1}{2i}\Lambda^{-1}A^T\overline{\alpha}} = \frac{1}{2i}\Lambda^{-1} \overline{\begin{bmatrix} A^{LR} & A^{RR} \\ A^{LL} & A^{RL} \end{bmatrix}^T \overline{\alpha}} \\ &= \frac{1}{2i}\Lambda^{-1} \overline{\begin{bmatrix} A^{RL} & A^{LL} \\ A^{RR} & A^{LR} \end{bmatrix}} \overline{\begin{bmatrix} \overline{\alpha}_+ \\ \overline{\alpha}_- \end{bmatrix}} = \frac{1}{2i}\Lambda^{-1} \overline{\begin{bmatrix} A^{RL}\overline{\alpha}_+ & A^{LL}\overline{\alpha}_- \\ A^{RR}\overline{\alpha}_+ & A^{LR}\overline{\alpha}_- \end{bmatrix}}. \end{aligned} \quad (5.5)$$

We introduce now the following flipping operator  $R : \mathbb{C}^{2N} \rightarrow \mathbb{C}^{2N}$  defined by:

$$R\alpha = [\alpha_{-1}, \alpha_{-2}, \dots, \alpha_{-N}, \alpha_1, \alpha_2, \dots, \alpha_N]^T = \begin{bmatrix} \alpha_- \\ \alpha_+ \end{bmatrix}. \quad (5.6)$$

One can verify easily that  $R$  has the following properties:

- (i)  $RR = I$
- (ii)  $\langle R\alpha, R\beta \rangle = \langle \alpha, \beta \rangle$
- (iii)  $R\overline{\alpha} = \overline{R\alpha}$
- (iv)  $R\Lambda = \Lambda R$  ( $R$  commutes with the diagonal matrix  $\Lambda$ ).

Using the flipping operator and its properties, we can rewrite equation (5.5) in a more compact form

$$\mathcal{A}^*\alpha = \overline{R\mathcal{A}R\overline{\alpha}}. \quad (5.7)$$

Using now (5.7), Lemma 1 and the properties of the flipping operator  $R$  again, we get

$$\begin{aligned} \langle \mathcal{A}^*\alpha, \mathcal{A}^*\beta \rangle &= \langle \overline{R\mathcal{A}R\overline{\alpha}}, \overline{R\mathcal{A}R\overline{\beta}} \rangle = \langle R\mathcal{A}R\overline{\beta}, R\mathcal{A}R\overline{\alpha} \rangle = \langle \mathcal{A}R\overline{\beta}, \mathcal{A}R\overline{\alpha} \rangle \\ &= -\langle R\overline{\beta}, \mathcal{A}R\overline{\alpha} \rangle = -\langle \mathcal{A}R\overline{\beta}, R\overline{\alpha} \rangle = -\langle \overline{\beta}, R\mathcal{A}R\overline{\alpha} \rangle = -\langle R\mathcal{A}R\overline{\beta}, \overline{\alpha} \rangle \\ &= -\langle \overline{R\mathcal{A}R\overline{\alpha}}, \overline{\beta} \rangle = -\langle \alpha, \overline{R\mathcal{A}R\overline{\beta}} \rangle = -\langle \mathcal{A}^*\alpha, \beta \rangle = -\langle \alpha, \mathcal{A}^*\beta \rangle \\ &= -\langle \alpha, \mathcal{A}\beta \rangle = -\langle \mathcal{A}\alpha, \beta \rangle \\ &= \langle \mathcal{A}\alpha, \mathcal{A}\beta \rangle. \end{aligned}$$

Since  $\langle \mathcal{A}^*\alpha, \mathcal{A}^*\beta \rangle = \langle \mathcal{A}\alpha, \mathcal{A}\beta \rangle$  for all the vectors  $\alpha, \beta \in \mathbb{C}^{2N}$ , it follows that  $\mathcal{A}\mathcal{A}^* = \mathcal{A}^*\mathcal{A}$ , that is  $\mathcal{A}$  is normal, and our proof is complete.

## 6. Inverse Method

Let us consider an incident wave distribution  $\alpha = \{\alpha_1, \alpha_2, \dots, \alpha_N, \alpha_{-1}, \alpha_{-2}, \dots, \alpha_{-N}\}^T$ ,  $\alpha \in \mathbb{C}^{2N}$ , for our waveguide problem. We define the following fields associated with  $\alpha$

$$E(x, z; \alpha) = \sum_{k=1}^N \alpha_k e^{i\sqrt{\lambda_k}x} \psi_k(z) + \sum_{k=1}^N \alpha_{-k} e^{-i\sqrt{\lambda_k}x} \psi_k(z) \quad \text{and} \quad (6.1)$$

$$F(x, z; \alpha) = \sum_{k=1}^N \alpha_k u_k(x, z) + \sum_{k=1}^N \alpha_{-k} u_{-k}(x, z), \quad (6.2)$$

which we call the *retransmitted field for the incident wave distribution  $\alpha$  in a homogeneous medium* and respectively the *retransmitted field for the incident wave distribution  $\alpha$  in an inhomogeneous medium*. Here  $u_k(x, z) = e^{i\sqrt{\lambda_k}x} \psi_k(z) + u_k^s(x, z)$  is the total field corresponding to the incident propagating mode  $u_k^i$ ,  $k = \pm 1, \dots, \pm N$ . It is worth mentioning the fact that the retransmitted fields  $E$  and  $F$  are not physical fields which we generate and send through the physical medium. They are just virtual fields that we obtain by taking linear combinations of the fundamental physical fields and which we use in our analysis and in our reconstruction algorithms.

Since the far-field matrix  $\mathcal{A}$  is normal with respect to the weighted inner product (5.2), it has a full complement of orthogonal eigenvectors. Let  $(\gamma_i, \alpha^i)$  be the  $2N$  eigenvalue-eigenvector pairs of  $\mathcal{A}$ , i.e.

$$\mathcal{A}\alpha^i = \gamma_i \alpha^i, \quad (6.3)$$

where to be consistent with our indexing convention,  $i = \pm 1, \pm 2, \dots, \pm N$ . In the following, we analyze the case when the retransmitted fields  $E$  and  $F$  correspond to incident wave distributions  $\alpha^i$  which are eigenvectors of the far-field matrix  $\mathcal{A}$ . In this case, we denote the corresponding retransmitted fields by  $E_i$  and respectively  $F_i$ .

Let us consider the  $k$ th component of equation (6.3), where  $k = 1, \dots, N$  is a positive index. Using definition (5.1) for  $\mathcal{A}$  we have

$$\gamma_i \alpha_k^i = [\gamma_i \alpha^i]_k = [\mathcal{A}\alpha^i]_k = \sum_{j=1}^N \frac{1}{2\sqrt{\lambda_k i}} (A_k^j \alpha_j^i + A_k^{-j} \alpha_{-j}^i),$$

and substituting  $A_k^j$  and  $A_k^{-j}$  by their formulas (3.3), we obtain

$$\gamma_i \alpha_k^i = \frac{1}{2\sqrt{\lambda_k i}} \int_{\Omega} e^{-i\sqrt{\lambda_k}X} \psi_k(Z) q(X, Z) F_i(X, Z) dX dZ. \quad (6.4)$$

Similarly, for the  $-k$ th component of equation (6.3),  $k = 1, \dots, N$ , we get

$$\gamma_i \alpha_{-k}^i = \frac{1}{2\sqrt{\lambda_k i}} \int_{\Omega} e^{i\sqrt{\lambda_k}X} \psi_k(Z) q(X, Z) F_i(X, Z) dX dZ. \quad (6.5)$$

Let  $\alpha^j$ ,  $j = \pm 1, \dots, \pm N$  be another eigenvector of  $\mathcal{A}$ . If we multiply (6.4) and (6.5) by  $\overline{\alpha_k^j}$  and respectively by  $\overline{\alpha_{-k}^j}$  and sum them up, we obtain

$$2i \langle \mathcal{A}\alpha^i, \alpha^j \rangle = 2i \gamma_i \delta_{ij} = \int_{\Omega} \overline{E}_j(X, Z) q(X, Z) F_i(X, Z) dX dZ, \quad (6.6)$$

for all  $i, j = 1, \dots, N, -1, \dots, -N$ , where  $\langle \cdot, \cdot \rangle$  represents the weighted inner product (5.2).

The system of equations (6.6) relates the eigenvalues  $\gamma_i$  of the far-field matrix  $\mathcal{A}$  to the variation in sound speed  $q$  together with the retransmitted fields  $E$  and  $F$

corresponding to incident wave distributions associated with the eigenvectors of  $\mathcal{A}$ . If we assume that we know the scattered fields from measurements, then we know the far-field matrix  $\mathcal{A}$  along with its eigenvalues and its eigenvectors. Therefore, equations (6.6) represent a starting point for an inverse method to determine the variation in the sound speed  $q$  from measurements of the scattered fields at the openings of the waveguide.

It is clear that the system of equations (6.6) cannot completely determine  $q$  which is a function, which in principle has an infinite number of unknowns. Instead, we regularize the problem and we look for a solution of (6.6) that minimizes the  $L^2$  norm on  $\Omega$ . Technically, this means that we look for a low-pass filtered version of  $q$ . So our inverse problem reduces to the following constrained optimization problem:

$$\min_q \|q\|^2 = \int_{\Omega} |q(X, Z)|^2 dX dZ \quad (6.7)$$

subject to

$$2i \langle \mathcal{A}\alpha^i, \alpha^j \rangle = 2i\gamma_i \delta_{ij} = \int_{\Omega} \overline{E_j}(X, Z) q(X, Z) F_i(X, Z) dX dZ, \quad (6.8)$$

for all  $i, j = 1, \dots, N, -1, \dots, -N$ .

At a minimum, the Frechet derivative of  $\|q\|^2$  is a linear combination of the Frechet derivatives of the constraints. The Frechet derivative of the objective function with respect to  $q$  is

$$d_q (\|q\|^2) [\tilde{q}] = \lim_{\varepsilon \rightarrow 0} \frac{\|q + \varepsilon \tilde{q}\|^2 - \|q\|^2}{\varepsilon} = 2 \int_{\Omega} q(X, Z) \tilde{q}(X, Z) dX dZ. \quad (6.9)$$

In order to compute the Frechet derivative of the constraints we interpret the terms in (6.8) in the following way: we compute the eigenvalues and the eigenvectors of the measured far-field matrix  $\mathcal{A}^{meas}$ , and we assume they are *fixed*. So, in (6.8), only  $\mathcal{A}$  depends on  $q$  and we look for  $q$  such that we have equality. Therefore when we compute the Frechet derivatives we obtain

$$d_q (2i \langle \mathcal{A}\alpha^i, \alpha^j \rangle - 2i\gamma_i \delta_{ij}) [\tilde{q}] = 2i \langle d_q \mathcal{A}[\tilde{q}] \alpha^i, \alpha^j \rangle. \quad (6.10)$$

In order to compute the Frechet derivative of  $\mathcal{A}$  with respect to  $q$  in (6.10), we need the following technical lemma, whose proof can be found in [6]:

**Lemma 2** *The following two-potential formulas hold for our waveguide problem:*

$$A_{\pm n}^{\pm m}(q_1) - A_{\pm n}^{\pm m}(q_2) = \int_{\Omega} u_{\pm m}^1(X, Z) [q_1(X, Z) - q_2(X, Z)] u_{\mp n}^2(X, Z) dX dZ$$

where:  $u^1$  and  $u^2$  are total fields corresponding to  $q_1$  and respectively  $q_2$  and  $A_{\pm n}^{\pm m}(q_1)$  and  $A_{\pm n}^{\pm m}(q_2)$  are coefficients of the scattering amplitudes corresponding to  $q_1$  and respectively  $q_2$ .

Using Lemma 2, the derivative of the constraints (6.8) with respect to  $q$  is:

$$d_q [\langle \mathcal{A}\alpha^i, \alpha^j \rangle - \delta_{ij}\gamma_i] [\tilde{q}] = \langle d_q \mathcal{A}[\tilde{q}] \alpha^i, \alpha^j \rangle = \frac{1}{2i} \int_{\Omega} F_i(X, Z) \tilde{q}(X, Z) \overline{F_j^*}(X, Z) dX dZ,$$

where  $\overline{F^*}(X, Z) = \sum_{k=1}^N \overline{\alpha_k^j} u_{-k}(X, Z) + \sum_{k=1}^N \overline{\alpha_{-k}^j} u_k(X, Z)$ . The optimality condition for the minimization problem (6.7)-(6.8) then implies

$$2 \int_{\Omega} q_M(X, Z) \tilde{q}(X, Z) dX dZ = \sum_{l \in J} \sum_{m \in J} Q_{lm} \int_{\Omega} F^l(X, Z) \tilde{q}(X, Z) \overline{F^{*m}}(X, Z) dX dZ,$$

where  $q_M$  is the optimal solution which minimizes the  $L^2$  norm and  $Q_{lm}$  are Lagrange multipliers. The set  $J$  in the equation above represents the ordered set of our indexes, i.e.  $J = \{1, \dots, N, -1, \dots, -N\}$ . Since the above equation is true for all  $\tilde{q}$ , we obtain

$$q_M(X, Z) = \sum_{l \in J} \sum_{m \in J} Q_{lm} F_l(X, Z) \bar{F}_m^*(X, Z). \quad (6.11)$$

We return now to the constraints (6.8) and ask  $q_M$  to satisfy them which implies

$$2i\gamma_i < \alpha^i, \alpha^j > = \int_{\Omega} \bar{E}_j(X, Z) \left[ \sum_{l \in J} \sum_{m \in J} Q_{lm} F_l(X, Z) \bar{F}_m^*(X, Z) \right] F_i(X, Z) dX dZ,$$

or equivalently

$$2i\gamma_i \delta_{ij} = \sum_{l \in J} \sum_{m \in J} \left[ \int_{\Omega} F_l(X, Z) \bar{E}_j(X, Z) F_l(X, Z) \bar{F}_m^*(X, Z) dX dZ \right] Q_{lm}, \quad (6.12)$$

for  $i, j = 1, \dots, N, -1, \dots, -N$ . If we have a good estimate for the total field  $u = u^i + u^s$ , we then would have good estimates for the retransmitted fields  $F$  and  $\bar{F}^*$ . Therefore we could in this case solve the linear system of equations (6.12) by standard numerical techniques for the coefficients  $Q_{lm}$ . Having these coefficients computed, we could then substitute them in equation (6.11) and we would get a reconstruction for the variation of the sound speed in the medium.

Although equation (6.11) expresses our regularized solution  $q_M$  in terms of products of retransmitted fields for the *inhomogeneous medium*, this representation is of limited use in practice since the retransmitted fields  $F_l$  and  $F_m$  for the inhomogeneous medium depend on the total field  $u$ , which is unknown in the rectangular region  $\Omega$ . However, in the case of a weak inhomogeneity (our assumption in this paper), arguably the scattered field can be neglected, and under what is called the Born approximation, the total field is approximated everywhere in the rectangular region  $\Omega$  by the incident field, i.e.

$$u_k(x, z) \approx e^{i\sqrt{\lambda_k}x} \psi_k(z),$$

for all  $k = \pm 1, \dots, \pm N$ . In this case, the representation (6.11) of the scattering potential takes the form

$$q_B(X, Z) = \sum_{l \in J} \sum_{m \in J} Q_{lm} E_l(X, Z) \bar{E}_m(X, Z), \quad (6.13)$$

where  $q_B$  is the linearized version of our regularized solution, and the problem of finding the unknown inhomogeneity reduces to the problem of solving the finite system of linear equations

$$2i\gamma_i \delta_{ij} = \sum_{l \in J} \sum_{m \in J} \left[ \int_{\Omega} E_i(X, Z) \bar{E}_j(X, Z) E_l(X, Z) \bar{E}_m(X, Z) dX dZ \right] Q_{lm}, \quad (6.14)$$

for the coefficients  $Q_{lm}$ . The coefficients in the finite system of linear equations above depend on the background medium and the eigenvalues and the eigenvectors of the far-field matrix. The double integrals in the linear system above can be decoupled as products of integrals in  $x$  and  $z$  directions which can be readily evaluated analytically when  $c(z)$  is independent of  $z$  or by standard numerical techniques when  $c(z)$  has  $z$  dependence.

We conclude this section with the important observation that in the numerical implementation of our inverse algorithm we never numerically solve the constrained optimization problem (6.7)-(6.8). Solving a constrained optimization problem in

practice is usually carried out by iterative algorithms which are time-consuming procedures. Instead, we use the analytic derivation of the optimality condition of this problem to obtain a representation for the linearized solution in terms of products of fields which are linear combinations of the propagating modes of the waveguide and eigenvectors of the far-field matrix. As we have seen in the analysis above, the problem of finding the unknown inhomogeneity reduces to a problem of determining some coefficients in a finite system of linear equations whose coefficients depend on the background medium and the eigenvalues and the eigenvectors of the measured far-field matrix. The integrals in these coefficients, whose integrands depend on the background medium can be pre-computed and stored, resulting in a *real-time* inversion algorithm.

## 7. Numerical Results

In order to get synthetic data and to apply our inverse algorithm, we need to solve first the direct problem, that is to solve the Helmholtz equation in the infinite waveguide slab with incident fields coming from the sides. Since our inverse problem is ill-posed, i.e. the solution can be unstable under data perturbations, it is crucial to begin with a very accurate solver for the direct problem from which to obtain reliable synthetic data.

Although nowadays there are very efficient numerical solvers for Helmholtz equation in bounded domains with classical boundary conditions, there is still a challenge to solve the Helmholtz equation numerically in unbounded domains with incoming incident fields and outgoing radiation conditions at infinity. The main difficulty arises at the numerical implementation of the so-called Dirichlet-to-Neumann (DtN) boundary conditions which have a *nonlocal character* and which are essential in reformulating a problem on an unbounded domain as an equivalent problem on a bounded one. We developed a *fourth order* finite differences solver for our direct problem which uses an implementation of these DtN boundary conditions based on equations (2.4) and (2.5). With the synthetic data obtained, we were able to check the reciprocity relation, the normality of the far-field matrix and to apply our inverse method to reconstruct the inhomogeneities present in the waveguide. Numerical tests presented in [6] illustrate the fourth order accuracy of our solver.

We start by considering a numerical experiment in a waveguide slab of depth  $D = 3$  which contains a *weak* inhomogeneity in the middle. The inhomogeneous region has an elliptical shape with the horizontal and vertical axis  $a = 2$  and respectively  $b = 1$ ; it is centered in the vertical direction but shifted one unit to the left in the horizontal direction (See Figure 2 B). The sound speed of the background medium is constant, the background wavenumber is  $k = \sqrt{50}$  which allows 7 propagating modes. The sound speed contrast inside the ellipse is varying smoothly from zero on the boundary to a maximum value of 2.5% of the background sound speed in the center. To get the synthetic data needed to apply our inverse algorithm, we solve the direct problem for each of the seven incident propagating modes coming from the sides. For the particular case of the 5<sup>th</sup> incident mode coming from the left to the right, this process is illustrated in Figure 2, where besides the incident field  $u^i$  and the scattering potential  $q$ , we also display the total field  $u$  and the scattered field  $u^s$ . Since in practice one knows the scattered field from measurements only on two vertical lines located at the openings of the waveguide, in our inversion algorithm we will use only the values of the scattered field sampled on the lines  $x = \pm L$ .

We compute the scattering amplitudes and the far-field matrix for our problem by using the asymptotic forms (3.2) of the scattered field. Our particular choice  $L = 4$  is large enough such that the exponential decay of the evanescent modes guarantees us a good agreement of the asymptotic expansions with the measured scattered fields.

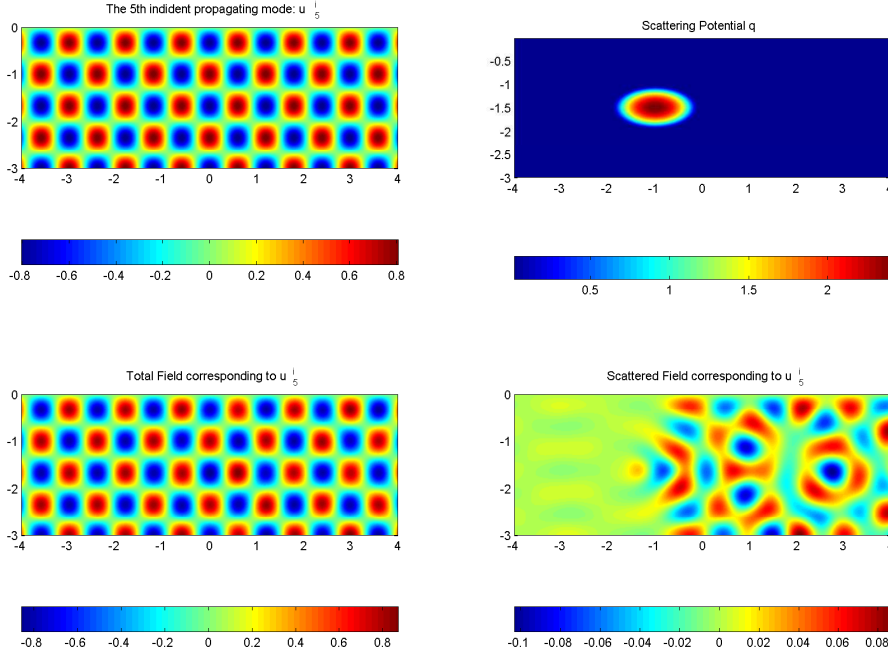


**Figure 2.** Wave Scattering in an acoustical waveguide: (A) Incident propagating mode  $u_5^i$  (B) Scattering Potential  $q$  (C) Total Field corresponding to  $u_5^i$  (D) Scattered Field corresponding to  $u_5^i$ .

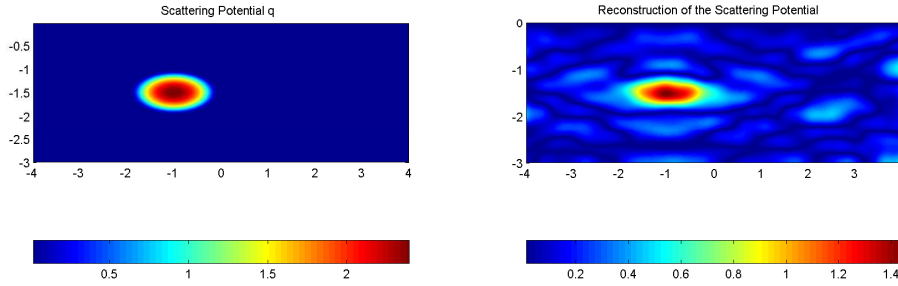
We obtained excellent numerical verification for the reciprocity relation satisfied by the scattering amplitude ( $1.70281 \cdot 10^{-6}$  accuracy in the reciprocity relation satisfied by the transmitted blocks,  $6.06414 \cdot 10^{-8}$  and  $6.06424 \cdot 10^{-8}$  accuracy for the reciprocity relation satisfied by the left and respectively by the right backscattered blocks) and for the normality of the far-field matrix ( $1.50888 \cdot 10^{-8}$  error from normality and  $1.34878 \cdot 10^{-6}$  error from the orthonormality of the eigenvectors). In Table 1 we present the transmitted parts for six scattering amplitudes corresponding to the 1<sup>st</sup> 3<sup>rd</sup> and 5<sup>th</sup> propagating modes from the left to the right and respectively 2<sup>nd</sup> 4<sup>th</sup> and 6<sup>th</sup> propagating modes from the right to the left. By visually inspecting these vectors, we corroborate that the reciprocity relation  $A_n^m = A_{-m}^{-n}$  for the scattering amplitude is verified.

In Figure 3 we present the numerical reconstruction of the inhomogeneous region obtained by using our eigensystem decomposition method. By comparing Figures 3 A and 3 B one observes that the inhomogeneity is well resolved and the center of the ellipse defined by the maximum magnitude is excellently recovered at  $(-1, -1.5)$ . The

**Table 1.** Checking the Reciprocity Relation  $A_n^m = A_{-m}^{-n}$  for the transmitted part of the Scattering Amplitude

$A^1$ (transmitted part)	$A^3$ (transmitted part)	$A^5$ (transmitted part)
0.5053 - 0.0358i	-0.4275 - 0.1858i	-0.0375 + 0.3012i
0.4587 - 0.1082i	-0.3654 - 0.0900i	0.0115 + 0.2065i
-0.3959 + 0.2462i	0.5090 - 0.0345i	-0.1432 - 0.4017i
-0.1632 + 0.3138i	0.2024 - 0.1465i	-0.1012 - 0.0753i
-0.0879 - 0.2905i	-0.0872 + 0.4174i	0.5130 - 0.0306i
-0.1186 - 0.0061i	0.0601 + 0.0319i	0.0055 - 0.0308i
0.0031 + 0.0107i	0.0040 + 0.0400i	0.1958 - 0.0620i
$A^{-2}$ (transmitted part)	$A^{-4}$ (transmitted part)	$A^{-6}$ (transmitted part)
0.4587 - 0.1082i	-0.1632 + 0.3138i	-0.1186 - 0.0061i
0.5063 - 0.0360i	-0.2739 + 0.3609i	-0.2060 - 0.0527i
-0.3654 - 0.0900i	0.2024 - 0.1465i	0.0601 + 0.0319i
-0.3243 - 0.3164i	0.5124 - 0.0345i	0.1600 + 0.3372i
0.0115 + 0.2065i	-0.1012 - 0.0753i	0.0055 - 0.0308i
-0.1916 + 0.0921i	0.1121 - 0.3560i	0.5222 - 0.0250i
0.0057 - 0.0235i	0.0164 + 0.0211i	-0.0126 + 0.0239i

shape and the support of the inhomogeneity are well reconstructed but a notable fact to mention is a loss in amplitude from 2.4093 in the original to 1.4506 in the reconstructed potential. In terms of percentiles, this represents a 60.21% recovery.


**Figure 3.** Reconstruction of a centrally located Scattering Potential: (A) Original (B) Reconstruction with 7 modes.

We considered next the cases when our inhomogeneity is located at the bottom and at the top of the waveguide. In order to compare the performances of our inverse algorithm for different locations within the waveguide, we keep all the parameters the same and change only the coordinates of the center of the ellipse. In Figure 4 we present the reconstruction for the case when our inhomogeneity is supported on half of an ellipse placed at the bottom, one unit shifted to the right. We note again that the location, the shape and the support of the inclusion are very well resolved and unlike the centered case we have a much better recovery in amplitude this time. In terms of numbers, the amplitude of the reconstruction at its maximum is 1.9960 versus 2.4093 in the original which yields a 82.85% recovery.

In Figure 5 we show the results for the case when our inhomogeneity is placed at

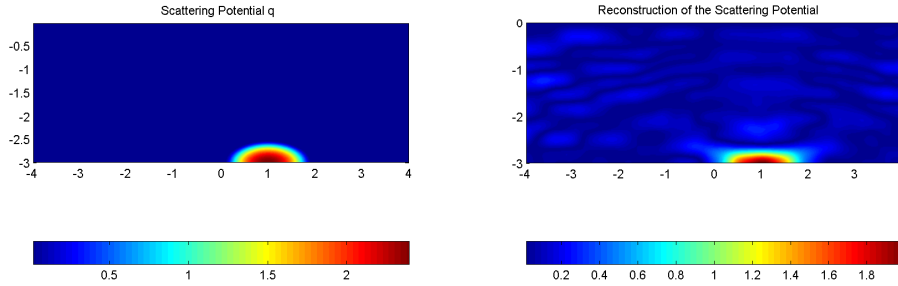


**Figure 4.** Reconstruction of the Scattering Potential: Bottom

the top of the waveguide, one unit shifted to the right and again supported on half of an ellipse. The location and the support of the inclusion are well resolved, but one interesting feature to note in this case is the fact that although the original inclusion is nonzero at the surface, the reconstruction is always zero there. This artifact is due to the eigenfunctions  $\psi_n$  which are zero at  $z = 0$  and which are utilized in our expansion (6.13) for  $q$ . Another important feature to note is the recovery in amplitude, which in this case is substantially more reduced than in the two previously considered cases.

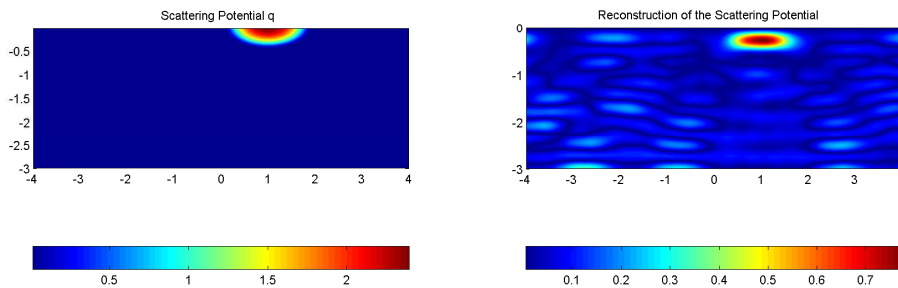


**Figure 5.** Reconstruction of the Scattering Potential: Top

In order to avoid technical difficulties in our analytical treatment of the problem, we assumed that the speed of sound is continuous, but we pointed out that this assumption doesn't represent an essential constraint. In order to support this affirmation made at the beginning of this paper, in Figure 6 we present numerical reconstructions (center and bottom) for a scattering potential which is piecewise constant and has a jump on the boundary of the inclusion. The geometry of the ellipse is the same as before but the sound speed contrast is 2.5% everywhere inside. We notice that again, we recover the shape and the size of the inclusion, but in this case the recovery in the amplitude is better than in the corresponding cases where we had a continuous scattering potential.

At this point we address the issue of analyzing what happens when we increase the

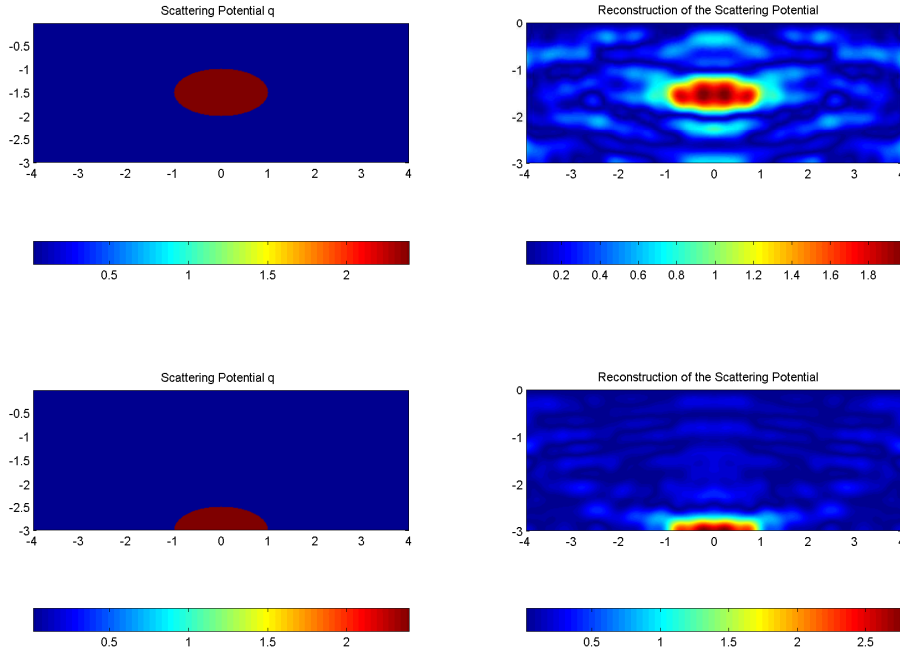


**Figure 6.** Reconstruction of a discontinuous Scattering Potential.

number of incident propagating modes. From the theory presented in Section 6 and on physical grounds, we expect to get better numerical reconstructions if we have a higher number of propagating modes, since in this case we have more information about the inhomogeneity contained in the far-field matrix. However in order to analyze and compare the numerical results corresponding to different numbers of propagating modes, first we need to normalize the reconstructed scattering potentials since they depend on the background wavenumber. We do this by fixing the first frequency  $\omega_0$  and then multiplying the scattering potential for a second frequency  $\omega_1$  by  $\omega_0^2/\omega_1^2$ . Numerical reconstructions for the same inhomogeneity when we have 7 and respectively 10 propagating modes are presented in Figure 7. We note that in both cases the inhomogeneity is well resolved and that the shape and the location are well recovered. In the case of the reconstruction with 10 modes, we note a better reconstruction of the support of the inhomogeneity which more closely follows the boundary of the ellipse. However, an important difference appears when we compare the amplitudes of the two reconstructions which are 1.4872 for the case of 7 modes and respectively 1.7887 for the case of the reconstruction with 10 modes. Compared to 2.4093 which is the amplitude of the original, these reconstructions represent 60.21% and respectively 74.17% recovery, which confirms our expectations that the reconstructions with a higher number of modes are better.

Next, we present numerical reconstructions for the more relevant case in Ocean Acoustics of flattened out inhomogeneities, whose horizontal dimensions are much larger than the vertical ones. In Figure 8 A we model such an inhomogeneity by an

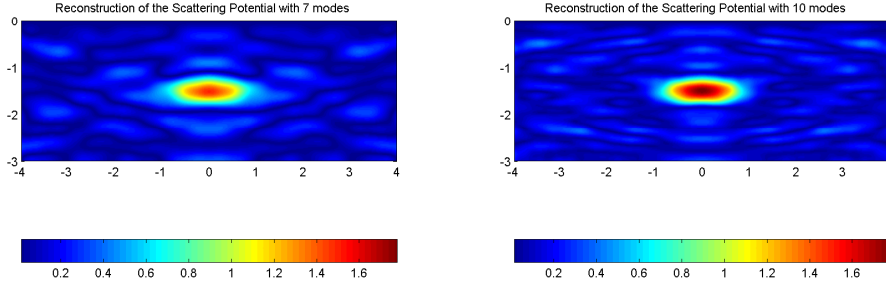


**Figure 7.** Reconstruction of the Scattering Potential: (A) with 7 modes; (B) with 10 modes.

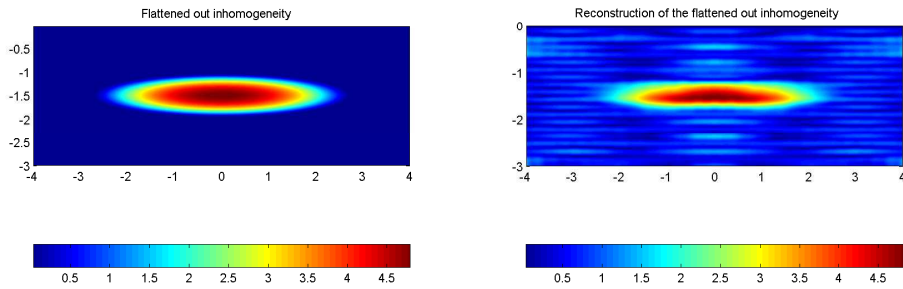


**Figure 8.** Reconstruction of Flattened Out Ellipse: (A) Original (B) Reconstruction with 10 modes.

elongated ellipse whose horizontal and vertical axis are  $a=6$  and  $b=1$ . The inclusion is fully supported inside the waveguide and centered both horizontally and vertically. The sound speed contrast varies smoothly from 0 on the boundary to 2.5% at its maximum in the center. In Figure 8 B we present the reconstruction obtained by using 10 propagating modes ( $k^2 = 100$ ). We note again that the the inhomogeneity is well resolved, and the shape and the location are well recovered.

So far, we have presented reconstructions only for the case when we have a single inhomogeneity present in the waveguide. In Figure 9 we present reconstructions for the case when we have two elliptical inhomogeneities supported inside the waveguide with centers at  $(-1.5, 1)$  and  $(1.5, -2.5)$  respectively, and we illuminate the waveguide with 10 propagating modes. The two ellipses are identical and have the same axis as before, i.e.  $a = 2$ ,  $b = 1$ . Our algorithm *doesn't need to know a priori the number of inhomogeneities* present in the waveguide and as one can notice, it reconstructs the support of each of them. The two inhomogeneities are well resolved and as expected the amplitude and the support of the one below are reconstructed slightly better than the amplitude and the support of the one above. Similar to our previous reconstructions the amplitude is reduced; in this case the amplitude of the reconstruction at its maximum is 3.5584 versus 4.8186 in the original, which yields a 73.85% recovery.

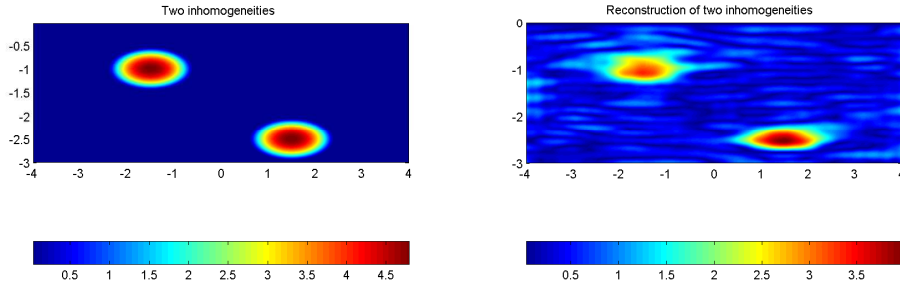


**Figure 9.** Reconstruction of two inhomogeneities: (A) Original (B) Reconstruction with 10 modes.

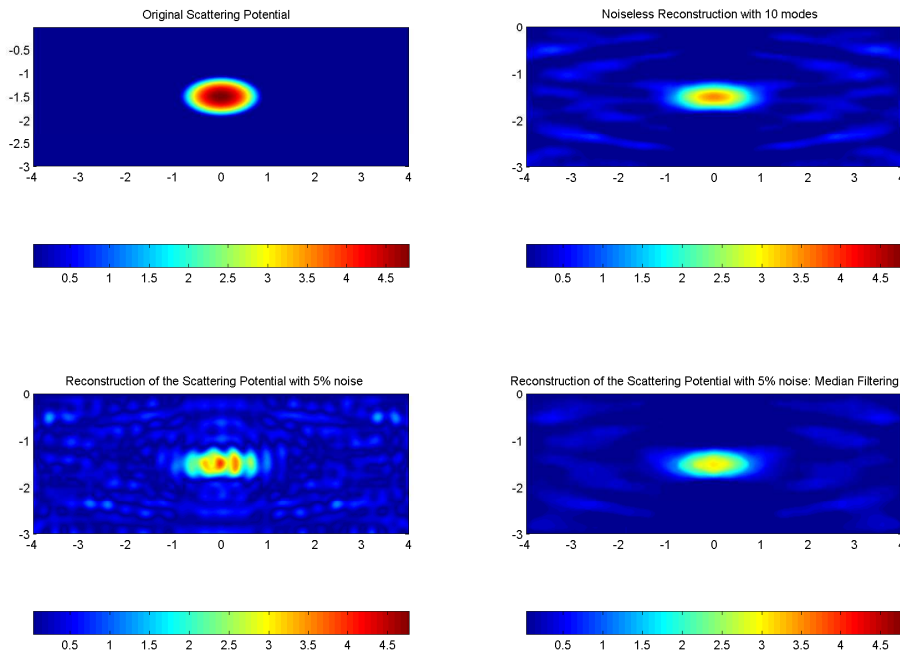


**Figure 10.** Reconstruction of an inhomogeneity with 10 modes and noisy scattered data: (A) Original, (B) Noiseless Reconstruction (C) Reconstruction with 5% added Gaussian Noise, (D) Median Filtered Enhancement of (C)

We conclude this section by presenting numerical reconstructions which suggest the stability of our inverse algorithm. Figure 10 shows the elliptical inhomogeneity and its reconstruction using scattering data as before but with 5% added Gaussian noise.

For comparison, in Figures 10 A and 10 B we present the original and respectively the noiseless reconstruction, and in Figure 10 C we present the reconstruction from noisy data as it results by using the same method as before and without any post-processing method used. In Figure 10 D we enhance the result presented in (C) by applying a median filter to our noisy reconstruction. Although featuring high-frequency artifacts, the reconstruction in (C) contains all the relevant information about the inhomogeneity we want to reconstruct. Up to a small loss in amplitude from 3.5319 to 3.1466, the median filtered version of our reconstruction shown in (D) is almost similar to the noiseless reconstruction.

## 8. Conclusions

An eigensystem decomposition method to recover inhomogeneities in a waveguide has been presented. Our method uses the eigenvalues and the eigenvectors of the far-field matrix to obtain a representation of the linearized solution to the inverse problem in terms of products of fields which are linear combinations of the propagating modes of the waveguide. The problem of finding the unknown inhomogeneity reduces to a problem of solving a finite system of linear equations whose coefficients depend on the background medium and the eigenvalues and the eigenvectors of the far-field matrix. We showed that the recoveries obtained with this method are good even when only a few propagating modes are used, of course improving as the number of propagating modes increases. In addition, by precomputing the integrals that depend only on the background medium this method results in a real time algorithm.

## Acknowledgments

We have benefitted from discussions with Jeong-Rock Yoon, Daniel Renzi and Donald Schwendeman from Rensselaer Polytechnic Institute which are acknowledged with pleasure. Funding for the work of SD was provided by the NFS Focus Group Grant DMS 0101458. JMcL was partially supported by NFS Focus Group Grant DMS 0101458, ONR Grants N000 14-96-1-0349 and N000 14-05-1-0600, and NIBIB Grant 1R21EB003000-01.

## References

- [1] Ahluwalia D., Keller J., Exact and asymptotic representations of the sound field in a stratified ocean. In *Wave Propagation and Underwater Acoustics*, pages 14-85. Lecture Notes in Physics 70. Springer-Verlag Berlin, 1977.
- [2] Buchanan J.L., Gilbert R.P., Wirgin A., and Xu Y., "Marine Acoustics, Direct and Inverse Problems", SIAM, 2004.
- [3] Colton D., Kress R., "Integral Equation Methodes in Scattering Theory", Wiley-Interscience Publication, New York, 1983.
- [4] Colton D., Kress R., "Inverse Acoustic and Electromagnetic Scattering Theory", Springer-Verlag, Berlin, 1992.
- [5] Colton D., Kress R., "Eigenvalues of the far field operator and inverse scattering theory", *SIAM J. Math. Anal.* 26, 601-615 (1995).
- [6] Dediu S., "Recovering inhomogeneities in a waveguide using eigensystem decomposition", Ph.D. Thesis, Rensselaer Polytechnic Institute, July 2005
- [7] Evans L.C., "Partial Differential Equations", American Mathematical Society, Providence, Rhode Island (1998).
- [8] Gilbert R. P., Xu Y., "Acoustic imaging in a shallow ocean with a thin ice cap", *Inverse Problems* 16, 2000.

- [9] Gilbert R.P., Mawata C., Xu Y., "Determination of a distributed inhomogeneity in a two-layered waveguide from scattered sound." In: R. Gilbert et al. (Eds.), *Direct and Inverse Problems of Mathematical Physics*. Kluwer Academic Publishers, Dordrecht, 2000.
- [10] Gilbert R.P., Werby M., Xu Y., "Determination of a buried object in a two-layered shallow ocean", *Journal of Computational Acoustics*, Vol. 9, No. 3, 1025-1037, 2001.
- [11] Givoli D., "Numerical methods for problems in infinite domains", in *Studies in Applied Mechanics*, Vol. 33, Elsevier, 1992.
- [12] Harari I., Patlashenko I., Givoli D., "Dirichlet-to-Neumann Maps for Unbounded Waveguides", *Journal of Computational Physics*, 143, 200-223, 1998.
- [13] Hewitt E., Stromberg K., "Real and Abstract Analysis", Springer-Verlag, Berlin, 1965.
- [14] Kirsch A., "An Introduction to the Mathematical Theory of Inverse Problems", Springer-Verlag, New York, 1996.
- [15] McLean W., "Strongly Elliptic Systems and Boundary Integral Equations", Cambridge University Press, 2000.
- [16] Morse P.M., Feshbach H., "Methods of Theoretical Physics", vol.1, McGraw-Hill Book Company, New York, 1953.
- [17] Mast T.D., Nachman A., Waag R., "Focusing and imaging using eigenfunctions of the scattered operator", *J. Acoust. Soc. Am.*, 102, 715-725, 1997.
- [18] Snieder R., "A Guided Tour of Mathematical Methods for the Physical Sciences", Cambridge University Press, 2001.
- [19] Strikwerda J.C., "Finite difference schemes and partial differential equations", Wadsworth & Brooks/Cole Advanced Books & Software, Pacific Grove, California, 1989.
- [20] Xu Y., "Radiation condition and scattering problem for time-harmonic acoustic waves in a stratified medium with non-stratified inhomogeneity", *IMA Journal of Applied Mathematics*, 54, 9-29, 1995.
- [21] Xu Y., "Inverse Acoustic Scattering Problems In Ocean Environments", *Journal of Computational Acoustics*, Vol. 7, No. 2, 111-132, 1999.